Available online at www.sciencedirect.com

SCIENCE DIRECT®

Earth and Planetary Science Letters 234 (2005) 235–248

EPSL

www.elsevier.com/locate/epsl

^{231}Pa and ^{230}Th in surface sediments of the Arctic Ocean: Implications for ^{231}Pa/^{230}Th fractionation, boundary scavenging, and advective export

S.B. Moran[a,*], C.-C. Shen[b], R.L. Edwards[c], H.N. Edmonds[d], J.C. Scholten[e], J.N. Smith[f], T.-L. Ku[g]

[a]*Graduate School of the Oceanography, University of Rhode Island, Narragansett, RI 02882-1197, USA*
[b]*Department of Geosciences, National Taiwan University, Taipei 106, Taiwan, R.O.C.*
[c]*Department of Geology and Geophysics, University of Minnesota, Minneapolis, MN 55455, USA*
[d]*Marine Science Institute, The University of Texas at Austin, Port Arkansas, TX 78373-5015, USA*
[e]*Institut fuer Geowissenschaften, Geologie, Universitat Kiel, Olshausentr. 40, D-24118 Kiel, Germany*
[f]*Marine and Environmental Sciences Division, Bedford Institute of Oceanography, Dartmouth, N.S., Canada B2Y 4A2*
[g]*Department of Earth Sciences, University of Southern California, Los Angeles CA 90089-0740, USA*

Received 14 May 2004; received in revised form 14 January 2005; accepted 15 February 2005
Available online 12 April 2005
Editor: E. Boyle

Abstract

Activities of ^{231}Pa and ^{230}Th in surface sediments from the Arctic Ocean and Greenland–Norwegian Seas are used to examine the redistribution of these water-column produced tracers between the low productivity interior basins and high particle flux marginal areas. Sediment $^{231}Pa_{xs}/^{230}Th_{xs}$ ratios throughout the Canadian and Eurasian Basins and the high particle flux Chukchi slope region are essentially invariant (average $= 0.063 \pm 0.014$, $N = 39$) and significantly below the water column production ratio (0.093). $^{231}Pa_{xs}/^{230}Th_{xs}$ ratios are also below the production ratio in the seasonally high productivity Greenland–Norwegian Sea basins (average $= 0.082 \pm 0.024$, $N = 13$), though they are ~ 30% higher than the interior Arctic. The low sediment $^{231}Pa_{xs}/^{230}Th_{xs}$ ratios are attributed to the net export of ~ 39% of dissolved ^{231}Pa produced in intermediate/deep waters, as opposed to ~ 10% of ^{230}Th, through Fram Strait. The negligible ^{230}Th export, combined with the reported low $^{230}Th_{xs}$ inventory of basin sediments and high $^{230}Th_{xs}$ inventory in Chukchi slope sediments, points to significant boundary scavenging of ^{230}Th in the Arctic. The invariant $^{231}Pa_{xs}/^{230}Th_{xs}$ ratios further indicate that scavenging of ^{230}Th is comparable to ^{231}Pa (i.e., fractionation to a similar degree between the two nuclides) in both the interior basins and margins. Thus, while significant boundary scavenging of both ^{231}Pa and ^{230}Th occurs in the Arctic, there is a distinct lack of basin-margin

* Corresponding author. Tel.: +1 401 874 6530; fax: +1 401 874 6811.
E-mail address: moran@gso.uri.edu (S.B. Moran).

0012-821X/$ - see front matter
doi:10.1016/j.epsl.2005.02.016

fractionation and a sizable export of ^{231}Pa. There is also likely to be export of other similarly particle-reactive radionuclides (e.g., ^{10}Be, Pu isotopes) out of the Arctic.

Keywords: Arctic; thorium-230; protactinium-231; shelf-basin exchange; scavenging

1. Introduction

^{231}Pa ($t_{1/2}$=32.8 kyr) and ^{230}Th ($t_{1/2}$=75.5 kyr) are particle-reactive radionuclides produced uniformly in the oceans by alpha decay of soluble ^{235}U and ^{234}U, respectively, at a constant initial ^{231}Pa/^{230}Th activity ratio of 0.093. The differential oceanic residence times of ^{231}Pa (~ 50–200 yr) and ^{230}Th (~ 20–40 yr) [1–3] strongly influence the sedimentary ^{231}Pa/^{230}Th deposition ratio on a basin-wide scale [4–6]. Chemical fractionation of these tracers in the ocean results from the preferential lateral transport of ^{231}Pa and its enhanced removal in areas of high particle flux (such as ocean boundaries), which is referred to as "boundary scavenging" [7–9].

In the Pacific, preferential boundary removal of ^{231}Pa relative to ^{230}Th is clearly evident and characterized by sediment excess ^{231}Pa/^{230}Th ratios (^{231}Pa$_{xs}$/^{230}Th$_{xs}$) that may exceed the production ratio in marginal areas [6,10–12]. In contrast, boundary scavenging of ^{231}Pa relative to ^{230}Th appears to be weakly expressed in the Atlantic [13]. Because the residence times of ^{231}Pa and Atlantic intermediate/deep waters are similar (~ 100–200 yr), there is a net southward transport by advection of ~ 50–70% of the water column production of ^{231}Pa that limits the preferential accumulation of ^{231}Pa in high particle flux regions [13–17]. North of 50°S in the Atlantic, excess ^{231}Pa/^{230}Th ratios in Holocene sediments [13], suspended particulate matter [15,16], and sediment trap material [18] all fall below the production ratio, consistent with model predictions [17]. This observation has generated significant interest in the application of excess sediment ^{231}Pa/^{230}Th as a paleocirculation tracer in the Atlantic. In addition to particle flux and water mass age, variations in particle composition can also alter oceanic and hence sedimentary ^{231}Pa/^{230}Th ratios [19–23]. In particular, ^{231}Pa is preferentially removed by biogenic opal [19,20,22,23], resulting in enhanced scavenging of ^{231}Pa transported southwards from the Atlantic and sedimentary ^{231}Pa/^{230}Th ratios in the Southern Ocean that exceed the production ratio [13,24,25].

Early studies of sedimentary ^{230}Th and ^{231}Pa [26] and ^{10}Be [27] in the central Arctic indicated that their sedimentary inventories were below the respective supply from the water column, which was attributed to the inefficiency of scavenging in the low productivity Arctic. In this paper, we investigate the imprint of ^{231}Pa/^{230}Th fractionation and boundary scavenging in the Arctic Ocean by combining new measurements of surface sediment ^{231}Pa$_{xs}$/^{230}Th$_{xs}$ from the Canadian Basin with previous data from the Arctic and the adjacent Greenland–Norwegian Sea basins [13,28,29]. An implication of this study is that ^{230}Th is largely removed by boundary scavenging, whereas nearly half of the ^{231}Pa produced in-situ is exported out of the Arctic.

2. Methods

Sediment samples were collected in August–September, 1994, at 19 locations in the Canadian Basin as part of the joint U.S.–Canada Arctic Ocean Section (AOS-94) expedition aboard the *C.C.G.S. Louis S. St. Laurent* (LSL) and *U.S.C.G.C. Polar Sea* (PS) (Fig. 1; Table 1). This transarctic expedition allowed for collection of samples from the Chukchi shelf and slope, the Makarov, Eurasian (Amundsen and Nansen) Basins, the Lomonosov and Medeleyev Ridges, and the Norwegian Sea. Sediments were collected from a range of water depths including the shelf (~ 40–50 m), slope (~ 1000–2500 m), deep-sea ridges (~ 1000–1500 m), and the central deep basins (>3000 m). In addition to the AOS-94 samples, surface sediments were also collected in May–June, 2002, at 8 locations near the Chukchi slope as part of the Shelf-Basin Interaction Phase II (SBI-II) program (Fig. 1; Table

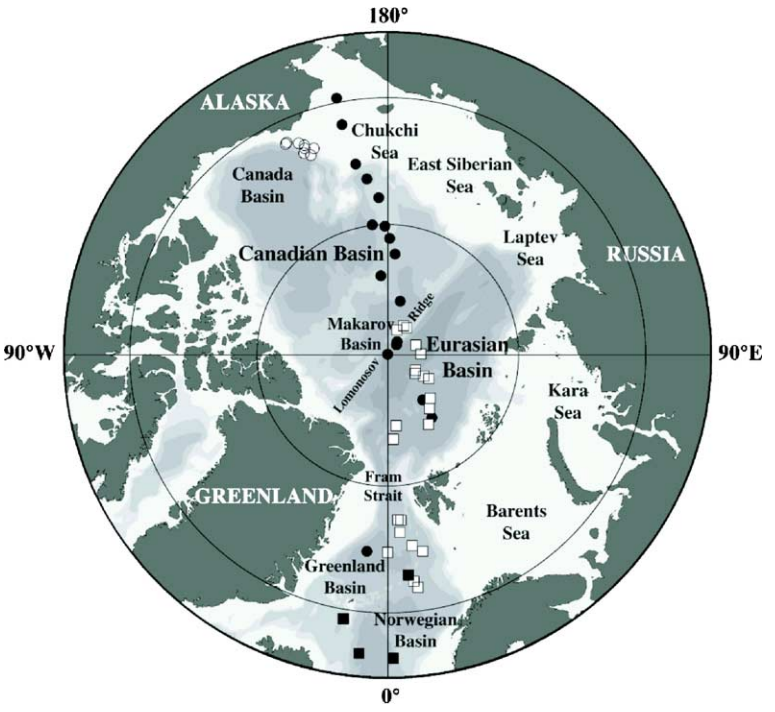

Fig. 1. Map of the Arctic Ocean and adjacent seas with station locations indicated for the 1994 Arctic Ocean Section (●), SBI-II (○), Scholten et al. [28] (□), and Yu et al. [13] (■).

1). Samples were collected from the Chukchi slope region and Canada Basin, which was not sampled during AOS-94. Box cores were used to collect sediments at all stations during AOS-94 and SBI-II. The box cores were subsampled at sea at 1 cm intervals. Surface sediments used for ^{231}Pa and ^{230}Th analysis are defined as the 0–1 cm interval. Sediment samples were stored frozen in plastic bags and returned to the laboratory for subsequent analysis.

The techniques used for chemical purification of sedimentary Pa, Th, and U in this study were based on those described for seawater analysis [30–32]. The carbonate fractions in sediment samples were first dissolved using 1 N HNO_3. The dissolved fraction was dried and redissolved with HNO_3–HCl–$HClO_4$ in capped Teflon beakers at 150 °C overnight. The residuals were dissolved with concentrated HF–HNO_3–$HClO_4$ in Teflon bombs at 108 °C for 24 h. Five drops of saturated H_3BO_3 were then added, dried down, and dissolved in 9 N HCl. The two digested fractions were combined in capped Teflon vials and refluxed to ensure a homogeneous solution. Two separate aliquots were taken for Pa and/or Th and U–Th analysis. The digested samples were then purified in a clean-room by anion-exchange [32].

^{231}Pa abundances were quantified using a Finnigan MAT 262 RPQ thermal ionization mass spectrometer in pulse counting mode [32]. ^{230}Th, ^{232}Th, ^{234}U, and ^{235}U abundances were measured using a Finnigan MAT ELEMENT sector-inductively coupled plasma mass spectrometer with a CETAC MCN-6000 sample introduction system [31]. Chemical blanks were 0.080 ± 0.040 fg for ^{231}Pa and 0.3 ± 0.1 fg for ^{230}Th, which correspond to 0.06–0.42% and 0.004–0.065% of the measured sample concentrations, respectively. Uncertainties in the ^{231}Pa, ^{230}Th, and ^{232}Th data were calculated at the 2σ level and include corrections for blanks, multiplier dark noise, abundance sensitivity, and the occurrence of ^{231}Pa, ^{230}Th and ^{232}Th in the ^{233}Pa and ^{229}Th spikes.

3. Results

Activities of U and Th isotopes, $^{231}Pa_{xs}$ and $^{231}Pa_{xs}/^{230}Th_{xs}$ activity ratios in surface sediments

Table 1
Activities of ^{238}U, ^{235}U, ^{234}U, ^{232}Th, $^{231}Pa_{xs}$, $^{230}Th_{xs}$, and $^{231}Pa_{xs}/^{230}Th_{xs}$ activity ratios in surface sediments of the Arctic Ocean

Area	Station	N. Lat.	Long.	Depth (m)	^{238}U[a] (dpm g^{-1})	^{235}U (dpm g^{-1})	^{234}U (dpm g^{-1})	^{232}Th (dpm g^{-1})	$^{231}Pa_{xs}$ (dpm g^{-1})	$^{230}Th_{xs}$ (dpm g^{-1})	$^{231}Pa_{xs}/^{230}Th_{xs}$ (activity ratio)
Arctic Ocean section, 1994											
Chukchi Shelf	LSL-2	72°08′	168°50′W	53	1.634 ± 0.005	0.075 ± 0.0002	1.555 ± 0.004	1.718 ± 0.017	0.042 ± 0.009	0.82 ± 0.19	0.052 ± 0.016
Chukchi Slope	LSL-11	76°38′	173°19′W	2227	1.856 ± 0.006	0.085 ± 0.0003	1.727 ± 0.005	2.332 ± 0.036	0.655 ± 0.025	13.07 ± 0.35	0.050 ± 0.002
Chukchi Slope	LSL-18	80°09′	173°15′W	2655	1.744 ± 0.007	0.080 ± 0.0003	1.611 ± 0.008	2.450 ± 0.055	1.246 ± 0.037	21.66 ± 0.38	0.058 ± 0.002
Makarov Basin	LSL-26	84°04′	175°04′E	3135	1.744 ± 0.005	0.080 ± 0.0002	1.603 ± 0.006	2.563 ± 0.083	1.157 ± 0.029	27.22 ± 0.45	0.043 ± 0.001
Amundsen Basin	LSL-35	90°00′	–	4215	1.690 ± 0.006	0.078 ± 0.0003	1.545 ± 0.006	2.615 ± 0.070	0.772 ± 0.035	17.36 ± 0.38	0.044 ± 0.002
Nansen Basin	LSL-36	85°44′	37°45′E	3471	1.676 ± 0.006	0.077 ± 0.0003	1.539 ± 0.006	2.554 ± 0.033	0.858 ± 0.047	16.90 ± 0.38	0.051 ± 0.003
Nansen Basin	LSL-37	84°15′	35°05′E	3979	1.696 ± 0.007	0.078 ± 0.0003	1.558 ± 0.006	2.848 ± 0.053	0.800 ± 0.030	17.89 ± 0.42	0.045 ± 0.002
Norwegian Sea	LSL-39	75°00′	6°03′W	3448	1.083 ± 0.005	0.050 ± 0.0002	0.994 ± 0.006	1.665 ± 0.030	0.280 ± 0.012	4.75 ± 0.20	0.059 ± 0.004
Chukchi Shelf	PS-1	70°00′	168°45′W	40	1.494 ± 0.008	0.069 ± 0.0003	1.441 ± 0.008	1.598 ± 0.023	0.031 ± 0.008	0.78 ± 0.18	0.039 ± 0.014
Chukchi Slope	PS-6	75°21′	170°30′W	525	1.864 ± 0.009	0.086 ± 0.0004	1.697 ± 0.009	2.705 ± 0.047	0.173 ± 0.018	2.27 ± 0.30	0.076 ± 0.013
	PS-8	78°08′	176°48′W	1047	1.718 ± 0.008	0.079 ± 0.0004	1.558 ± 0.007	2.697 ± 0.046	0.371 ± 0.021	5.26 ± 0.31	0.071 ± 0.006
	PS-13	80°09′	173°17′W	2654	1.612 ± 0.005	0.074 ± 0.0002	1.487 ± 0.005	2.383 ± 0.072	1.140 ± 0.048	18.63 ± 0.36	0.061 ± 0.003
Mendeleyev Ridge	PS-16	80°20′	178°43′W	1568	1.666 ± 0.005	0.077 ± 0.0002	1.527 ± 0.004	2.375 ± 0.040	0.826 ± 0.024	9.39 ± 0.28	0.088 ± 0.004
	PS-17	81°15′	179°00′E	2255	1.829 ± 0.005	0.084 ± 0.0003	1.681 ± 0.005	2.659 ± 0.073	0.923 ± 0.022	16.26 ± 0.35	0.057 ± 0.002
Makarov Basin	PS-19	82°26′	175°50′E	2414	1.747 ± 0.007	0.080 ± 0.0003	1.602 ± 0.009	2.497 ± 0.042	0.915 ± 0.020	17.85 ± 0.35	0.051 ± 0.001
	PS-23	85°54′	166°50′E	3535	1.516 ± 0.004	0.070 ± 0.0002	1.386 ± 0.004	2.146 ± 0.039	0.859 ± 0.026	17.44 ± 0.33	0.049 ± 0.002
Lomonosov Ridge	PS-26	88°48′	143°29′E	1034	1.553 ± 0.004	0.072 ± 0.0002	1.417 ± 0.004	2.308 ± 0.037	0.481 ± 0.020	6.20 ± 0.27	0.078 ± 0.005
Amundsen Basin	PS-30-1	89°01′	137°41′E	4064	1.725 ± 0.005	0.079 ± 0.0002	1.574 ± 0.003	2.622 ± 0.061	0.706 ± 0.021	12.12 ± 0.32	0.058 ± 0.002
Shelf-Basin Interaction-II, 2002											
Chukchi Slope	9-WHS5	73°21.35′	160°22.81′W	1151	2.314 ± 0.006	0.107 ± 0.0003	2.286 ± 0.006	2.101 ± 0.011	0.127 ± 0.011	1.86 ± 0.22	0.068 ± 0.010
	32-BC5	72°06.52′	154°36.75′W	1690	1.633 ± 0.003	0.075 ± 0.0002	1.483 ± 0.003	1.831 ± 0.011	0.075 ± 0.009	1.13 ± 0.20	0.066 ± 0.014
	16-EHS7	72°52.40′	158°21.67′W	1017	2.018 ± 0.004	0.093 ± 0.0002	1.950 ± 0.003	2.099 ± 0.013	0.064 ± 0.011	1.15 ± 0.22	0.055 ± 0.014
	14-EHS9	73°05.47′	158°10.93′W	2152	1.679 ± 0.003	0.077 ± 0.0001	1.580 ± 0.003	2.044 ± 0.016	0.042 ± 0.010	0.76 ± 0.22	0.056 ± 0.020
	33-BC6	72°10.91′	154°16.20′W	1975	1.745 ± 0.004	0.080 ± 0.0002	1.590 ± 0.004	1.986 ± 0.010	0.083 ± 0.010	1.27 ± 0.21	0.066 ± 0.014
Canada Basin	12-EHS11	73°26.26′	157°32.11′W	2855	1.750 ± 0.004	0.081 ± 0.0002	1.608 ± 0.004	2.205 ± 0.012	0.385 ± 0.012	6.90 ± 0.25	0.056 ± 0.003
	11-WHS7	73°46.56′	159°03.08′W	3124	1.940 ± 0.004	0.089 ± 0.0002	1.781 ± 0.004	2.479 ± 0.012	0.548 ± 0.017	9.81 ± 0.28	0.056 ± 0.002
	34-BC7	72°33.64′	157°11.46′W	2907	1.814 ± 0.004	0.084 ± 0.0002	1.664 ± 0.004	2.288 ± 0.013	0.166 ± 0.011	2.76 ± 0.24	0.060 ± 0.007

LSL—Louis S. St. Laurent stations; PS—Polar Sea stations.
[a] ^{238}U calculated from measurement of ^{235}U and assumed $^{235}U/^{238}U$ activity ratio of 0.04605.

from stations occupied during the AOS-94 and SBI-II cruises are listed in Table 1. Note that ^{238}U activities were calculated as the quotient of the measured ^{235}U activity divided by the ^{235}U/^{238}U activity ratio, assumed to be 0.04605. The measured activities of ^{231}Pa and ^{230}Th were corrected for detrital, U-supported ^{231}Pa and ^{230}Th, which are assumed to be in secular equilibrium with ^{235}U and ^{234}U, respectively. The unsupported $^{231}Pa_{xs}$ and $^{230}Th_{xs}$ activities were calculated according to [33],

$$^{230}Th_{xs} = ^{230}Th_m - (0.6 \pm 0.1)^{232}Th_m \quad (1)$$

and

$$^{231}Pa_{xs} = ^{231}Pa_m - 0.04605(0.6 \pm 0.1)^{232}Th_m \quad (2)$$

where the subscript *m* represents the measured activity, 0.6 is an average detrital ^{238}U/^{232}Th activity ratio, and 0.04605 is the ^{235}U/^{238}U activity ratio in detrital material. The average detrital ^{238}U/^{232}Th activity ratio is similar to the average ^{238}U/^{232}Th ratio of 0.71 ± 0.09 measured in these Arctic surface sediments, and compares with values of 0.6 ± 0.1 for the Atlantic Ocean, 0.7 ± 0.1 for the Pacific Ocean, and 0.4 ± 0.1 south of the Antarctic Polar Front [33].

4. Discussion

4.1. Distributions of surface sediment $^{231}Pa_{xs}$, $^{230}Th_{xs}$, and $^{231}Pa_{xs}/^{230}Th_{xs}$ activity ratios

Surface sediment $^{231}Pa_{xs}$ and $^{230}Th_{xs}$ activities vary widely throughout the central Arctic and adjacent Greenland–Norwegian Sea, showing ranges of 0.031–1.246 dpm g^{-1} and 0.76–27.22 dpm g^{-1}, respectively (Fig. 2). For both $^{231}Pa_{xs}$ and $^{230}Th_{xs}$, the highest activities are generally observed in the deep central Arctic basins compared to the shelf and slope sediments of the Chukchi Sea and the Norwegian Sea basin. These activities are similar to previously reported values in core tops from the Canadian Basin

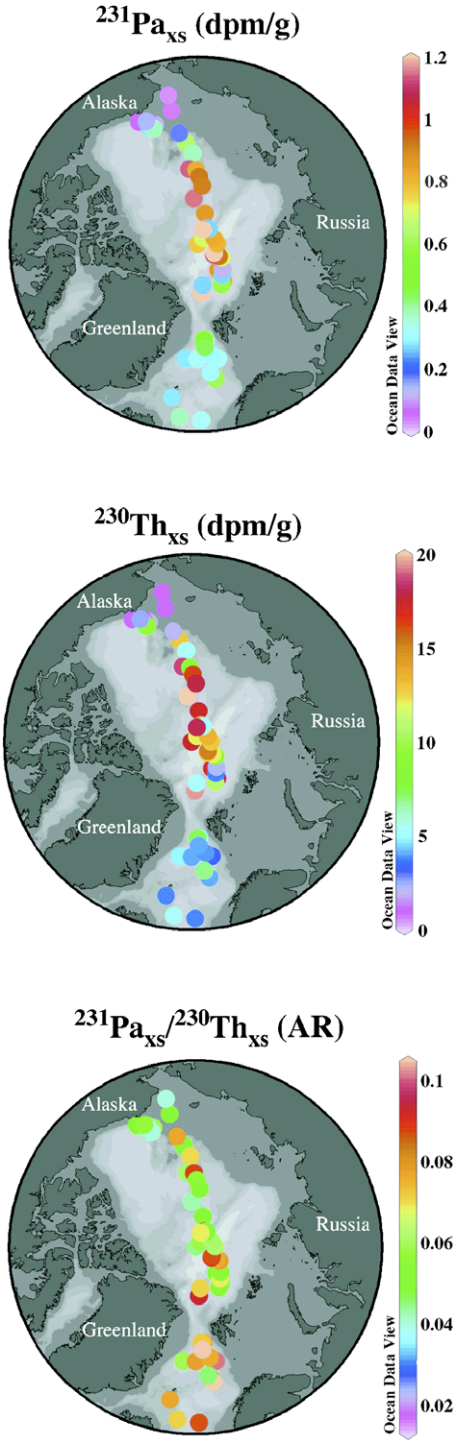

Fig. 2. Spatial distribution of $^{231}Pa_{xs}$ and $^{230}Th_{xs}$ activity and $^{231}Pa_{xs}/^{230}Th_{xs}$ activity ratios in surface sediments of the central Arctic Ocean and the Greenland–Norwegian Sea basins. Maps include radiochemical data reported in this study and from previous workers [13,28].

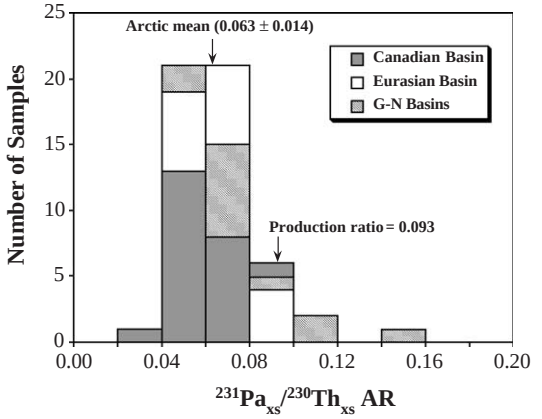

Fig. 3. Histogram of $^{231}Pa_{xs}/^{230}Th_{xs}$ activity ratios in surface sediments from the Canadian and Eurasian Basins of the central Arctic Ocean and the Greenland–Norwegian Sea basins (G–N Basins). Data include $^{231}Pa_{xs}/^{230}Th_{xs}$ ratios reported in this study and from previous workers [13,28].

[29]. The general pattern of higher activities in the low productivity, permanently ice-covered interior Arctic compared to the high productivity, high particle flux marginal regions is consistent with the inverse relationship between the excess sediment activity of these tracers and sediment accumulation rate in the Pacific [10]. Activities of $^{231}Pa_{xs}$ and $^{230}Th_{xs}$ in Arctic surface sediments are considerably lower (5–6 times) than in the Pacific, however, and closer to values in the Atlantic of 0.2–1 dpm g^{-1} and 1–12 dpm g^{-1}, respectively [34], even though Arctic sedimentation rates are generally closer to rates in the Pacific than in the Atlantic. Water column activities of ^{231}Pa and ^{230}Th are also generally lower in the Arctic [3,35] than the Pacific [2,36], though similar in magnitude to the Atlantic [14–16,37].

In contrast to the wide variation in surface sediment $^{231}Pa_{xs}$ and $^{230}Th_{xs}$ activities, the distribution of the sediment $^{231}Pa_{xs}/^{230}Th_{xs}$ ratio falls within a relatively narrow range on a Pan-Arctic basis (Fig 2). $^{231}Pa_{xs}/^{230}Th_{xs}$ ratios in surface sediments of the Canadian and Eurasian Basins are below the production ratio of 0.093, ranging from 0.039–0.088 (Fig. 3). The average surface sediment $^{231}Pa_{xs}/^{230}Th_{xs}$ ratio for the entire central Arctic (Canadian and Eurasian Basins) is 0.063 ± 0.014 (N=39), which is 68% of the production ratio (53–83% using the lower and upper limits of the stated uncertainty). This is also evident from the plot of $^{231}Pa_{xs}$ versus $^{230}Th_{xs}$, in which many samples fall below the production ratio (Fig. 4). Average $^{231}Pa_{xs}/^{230}Th_{xs}$ ratios in the Canadian Basin (0.060 ± 0.012, N=23) and Eurasian Basin (0.067 ± 0.016, N=16) are also lower than in the more productive Greenland–Norwegian basins (0.082 ± 0.024, N=13). There is clearly a basin-wide chemical fractionation, however, there is no significant $^{231}Pa/^{230}Th$ fractionation between the interior basin and margin regions. The salient feature of these data is the essentially invariant and low sediment $^{231}Pa_{xs}/^{230}Th_{xs}$ ratios throughout the low productivity interior Arctic and the high particle flux marginal areas of the Chukchi slope.

Because of the very low sediment accumulation rates typical of the Canadian Basin (0.1–0.3 cm kyr^{-1} [26,29]), it is important to consider whether low surface sediment $^{231}Pa_{xs}/^{230}Th_{xs}$ ratios result from sediment mixing via bioturbation [10]. Based on $^{210}Pb_{xs}$ data [38] from the Canadian Basin, bioturbation depths were estimated at ca. 3 cm. More recent work suggests that the mixed layer depth can range by 2–10 cm [39]. The effect of bioturbation on surface sediment $^{231}Pa_{xs}/^{230}Th_{xs}$ can be investigated using a simple box model such as those developed using ^{14}C [40,41]. Assuming a homogeneous mixed layer of

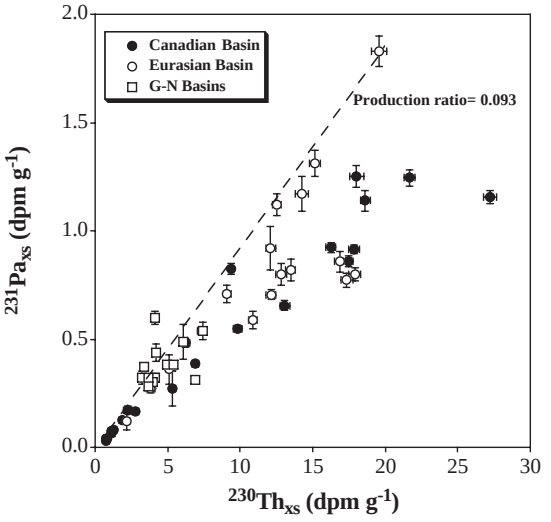

Fig. 4. Plot of $^{231}Pa_{xs}$ against $^{230}Th_{xs}$ in surface sediments from the Canadian and Eurasian Basins of the central Arctic Ocean and the Greenland–Norwegian Sea (G–N Basins) basins. Data include $^{231}Pa_{xs}$ and $^{230}Th_{xs}$ activities determined in this study and from previous workers [13,28].

depth M (cm), the activity of $^{230}Th_{xs}$ or $^{231}Pa_{xs}$ in the mixed layer can be expressed as,

$$A_{ML} = A_{rain}\left(\frac{1}{1+\lambda M/S}\right) \quad (3)$$

and for the $^{231}Pa_{xs}/^{230}Th_{xs}$ ratio,

$$R_{ML} = R_{rain}\left(\frac{S+\lambda_{Th}M}{S+\lambda_{Pa}M}\right) \quad (4)$$

where S is the linear sedimentation rate (cm yr^{-1}), R is $^{231}Pa_{xs}/^{230}Th_{xs}$ activity ratio, λ_{Th} and λ_{Pa} are the decay constants of ^{230}Th (9.19×10^{-6} yr^{-1}) and ^{231}Pa (2.17×10^{-5} yr^{-1}), and the subscripts ML and rain refer to activities or activity ratios in the mixed layer and in sedimenting material, respectively.

The resulting mixed layer $^{231}Pa_{xs}/^{230}Th_{xs}$ ratios as a function of sedimentation rate and mixed layer depth are depicted in Fig. 5. Reduction of the surface $^{231}Pa_{xs}/^{230}Th_{xs}$ ratio increases with increasing mixed layer depth and decreasing sedimentation rate. For typical central Arctic sedimentation rates of 0.1–0.3 cm kyr^{-1} [26,29] and mixed layer depths of 1–3 cm [38], a $^{231}Pa_{xs}/^{230}Th_{xs}$ rain ratio equal to the production ratio can be reduced to between 0.072 (S=0.1 cm kyr^{-1}, M=3 cm) and 0.089 (S=0.3 cm kyr^{-1}, M=1 cm). This relationship indicates that bioturbation may contribute to the low $^{231}Pa_{xs}/^{230}Th_{xs}$ ratios in very slowly accumulating Canadian Basin sediments; however, it is unlikely to account for the low $^{231}Pa/^{230}Th$ ratios on a Pan-Arctic basis.

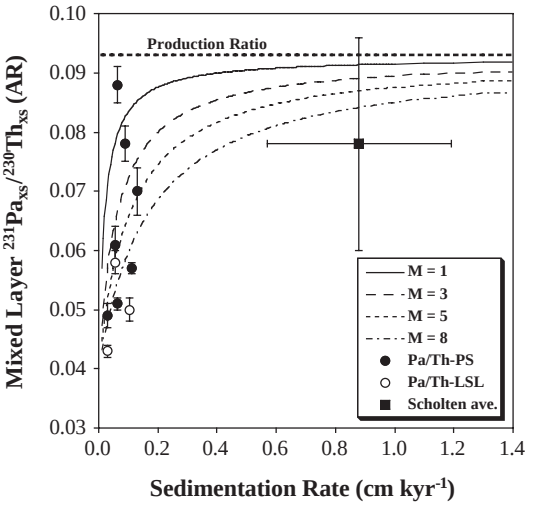

Fig. 5. Surface sediment $^{231}Pa_{xs}/^{230}Th_{xs}$ ratios from the Polar Sea (PS) and Louis St. Laurent (LSL) cruises in the Canadian Basin plotted against $^{230}Th_{xs}$-derived linear sedimentation rates reported for these same locations [29]. Also plotted is the average surface sediment $^{231}Pa_{xs}/^{230}Th_{xs}$ ratio from the Eurasian and Norwegian Sea basins (Scholten ave.; N=8 [28]) against the corresponding sedimentation rate obtained from the literature [64–67]. Lines calculated using a steady-state box model with variable bioturbation mixed layer thickness (M) (Eq. (4)). Sediment $^{231}Pa_{xs}/^{230}Th_{xs}$ ratios in the mixed layer decrease with both a decrease in sedimentation rate (most significantly below ~ 0.2 cm kyr^{-1}) and depth of sediment bioturbation.

4.2. Boundary scavenging

Boundary scavenging might be expected to be pronounced in the Arctic, owing to the combined effects of the unusually high proportion of shelf area (36%), the very low sediment accumulation rates and hence particle flux in the ice-covered interior basins, the large seasonal variations in productivity in the marginal regions [42–46] and the associated particle flux [47–51], the regional extremes in water mass age [52], and a dynamic circulation characterized by significant lateral mixing [53]. Indeed, early studies in the deep Canada Basin revealed sediment inventories of ^{231}Pa and ^{230}Th below their respective supplies by production in the overlying water column [26], an observation consistent with subsequent measurements of sedimentary ^{10}Be [27]. More recent observations indicate higher sediment inventories compared to the respective water column inventories of $^{210}Pb_{xs}$ and, to a lesser extent, $^{230}Th_{xs}$, in the Chukchi slope than in the interior Canadian Basin [29,39]. Water column distributions of ^{231}Pa and ^{230}Th in the Arctic exhibit wide spatial variations in these tracer concentrations and respective scavenging rates, with high rates near the margin of the Canada Basin [3,28,35,54]. Taken together, these observations indicate that these radionuclides are redistributed within the Arctic by horizontal mixing and preferentially removed in high productivity marginal areas, such as the Chukchi slope.

Initial studies of surface sediment $^{231}Pa_{xs}/^{230}Th_{xs}$ in the Eurasian Basin and the more productive Greenland–Norwegian Sea revealed values below the production ratio and no strong evidence of chemical fractionation between these two regions [28]. This is consistent with the short renewal time (decadal) of the intermediate waters [55] and Eurasian

Basin Deep Water (~ 50–60 yr) [56]. In the Canada Basin, which has a longer deep/bottom water renewal time of ~500 yr [57,58] and greater evidence of intra-basin variations in water column ^{230}Th and ^{231}Pa concentrations than the Eurasian Basin, there is also little evidence of shelf-basin variability in sediment $^{231}Pa_{xs}/^{230}Th_{xs}$. In addition, the water column $^{231}Pa/^{230}Th$ ratio is enriched in ^{231}Pa relative to the production ratio [3,28,35]. If water was to flow over the high-particle flux slope regions and lose congruent parts of both inventories (i.e., no preferential scavenging of ^{231}Pa relative to ^{230}Th), then this boundary scavenging would give rise to high $^{231}Pa_{xs}/^{230}Th_{xs}$ in marginal sediments without changing the water column $^{231}Pa/^{230}Th$ ratio. The salient point, however, is that $^{231}Pa_{xs}/^{230}Th_{xs}$ is below the production ratio and remarkably invariant in the sediment (Fig. 2).

We attribute the low sediment $^{231}Pa_{xs}/^{230}Th_{xs}$ ratios observed throughout the Arctic to chemical fractionation of ^{231}Pa and ^{230}Th in the water column combined with the preferential export by advection of ^{231}Pa from the Arctic. As in the Pacific [10], it might be expected that boundary scavenging would result in $^{231}Pa_{xs}/^{230}Th_{xs}$ ratios similar to, or possibly greater than, the production ratio in high particle flux margins, such as the Chukchi slope. This is an area characterized by some of the highest rates of biological production and particle flux in the world ocean [43], an environmental setting that would typically favor boundary scavenging. Indeed, Smith et al. [39] recently reported boundary scavenging of $^{210}Pb_{xs}$ in some of the same sediment samples analyzed in this study for $^{231}Pa_{xs}$ and $^{230}Th_{xs}$. Huh et al. [29] also reported boundary scavenging of $^{210}Pb_{xs}$ and $^{230}Th_{xs}$ in sediment cores from this region. These workers reported that the sediment inventory of $^{210}Pb_{xs}$ exceeded the supply from the overlying water column near the slope and shelves and that sediment $^{230}Th_{xs}$ inventories are greater in the margins than the interior basins.

The average $^{231}Pa_{xs}/^{230}Th_{xs}$ ratio determined in 10 samples collected from the Chukchi slope is only 0.063 ± 0.008. It is important to note, however, that while the Chukchi slope is a high particle flux area, this data set may not be representative of boundary regions in the Arctic as a whole. The distribution of sampling points is largely along the 0–180° axis of the Arctic and the coverage in the 90°E–90°W direction is limited (Fig. 1). It remains to be shown to what extent the low sediment $^{231}Pa_{xs}/^{230}Th_{xs}$ ratios and lack of basin-to-margin fractionation evident from these data exist for other slope/marginal areas of the Arctic. Regardless, with the exception of just one sample from the Mendeleyev Ridge (PS-16), preferential scavenging of ^{231}Pa is evidently insufficient to increase sediment $^{231}Pa_{xs}/^{230}Th_{xs}$ ratios to values that approach and/or exceed the production ratio in the high particle flux margins of the Arctic, as observed in the Pacific [10].

The mean Arctic $^{231}Pa_{xs}/^{230}Th_{xs}$ ratio (0.063 ± 0.014) is indistinguishable from the mean ratio of 0.060 ± 0.004 reported for the Atlantic, where low sediment $^{231}Pa_{xs}/^{230}Th_{xs}$ ratios have been attributed to the export of ^{231}Pa in southward flowing intermediate/deep waters [13,16,17]. We suggest that a similar situation exists in the Arctic, which is characterized by residence times of intermediate/deep waters typically on the order of ~ 50–100 yr [55,56], similar to the residence time of ^{231}Pa of ~ 110–200 yr [3,35]. Both the low sediment $^{231}Pa_{xs}/^{230}Th_{xs}$ ratios and lack of basin-margin $^{231}Pa_{xs}/^{230}Th_{xs}$ fractionation may be a result of the similar residence time of ^{231}Pa and Arctic intermediate/deep waters.

The lack of $^{231}Pa_{xs}/^{230}Th_{xs}$ fractionation between the margin and interior Arctic sediments does not mean that there is no boundary scavenging of ^{231}Pa in the Arctic. Rather, this may occur if the degree of boundary scavenging of ^{231}Pa is comparable to that of ^{230}Th. This is possible when: (1) scavenging of ^{231}Pa and ^{230}Th in the margins and interior Arctic is controlled mainly by the same mineral phases (e.g., lithogenic detritus [21]); and (2) the rate of lateral mixing is sufficiently fast that the dissolved $^{231}Pa/^{230}Th$ ratio in slope waters is similar to that in the interior basin [35].

Unlike the Atlantic, where sediment $^{231}Pa_{xs}/^{230}Th_{xs}$ ratios that exceed the production ratio are found in the high particle flux, high opal region south of 50°S, such elevated $^{231}Pa_{xs}/^{230}Th_{xs}$ ratios are not observed in any region of the Arctic sampled to date. As one expects there is no ^{230}Th in excess of the production rate in the water column, the question arises: where is the missing $^{231}Pa_{xs}$ that is required to balance the radiochemical budget in the Arctic Ocean? As noted above, it is possible that the missing ^{231}Pa may be preserved in high particle flux regions that have yet to be

sampled, such as the vast Eurasian slope/shelf area. We might have expected to find evidence for high ratios $^{231}Pa_{xs}/^{230}Th_{xs}$ due to boundary scavenging of ^{231}Pa in the productive Chukchi slope, though this is not the case (Fig. 2). The increase in surface sediment $^{231}Pa_{xs}/^{230}Th_{xs}$ towards the production ratio in the Greenland–Norwegian Sea suggests that scavenging of ^{231}Pa may be focused in this high productivity region, however, the average sediment $^{231}Pa_{xs}/^{230}Th_{xs}$ ratio is still below the production ratio. Finally, there is the possibility that ^{231}Pa is exported to the North Atlantic.

4.3. Export of dissolved ^{230}Th and ^{231}Pa from the Arctic Ocean

Several previous studies [26,27,54] have proposed that there may be a net export of particle-reactive radionuclides to the North Atlantic. The relative importance of basin-wide scavenging versus export of dissolved ^{231}Pa and ^{230}Th from the Arctic can be estimated using a simple 2-box model (Fig. 6) that compares the in-situ production of these tracers with their transport by advection through Fram Strait. This model builds on our recent water column studies [35] by inclusion of the more extensive sediment $^{231}Pa_{xs}/^{230}Th_{xs}$ data that call for an export of ^{231}Pa from the Arctic Ocean.

Export through the shallow passages of the Canadian Archipelago is not considered important as the upper waters (<200 m) transported through this region are characterized by low dissolved ^{231}Pa and ^{230}Th activities. Similarly, input of ^{231}Pa and ^{230}Th through the shallow Bering Strait is expected to be insignificant. Input of ^{231}Pa and ^{230}Th in upper waters from the Atlantic to the Arctic is also expected to be low due to low dissolved ^{231}Pa and ^{230}Th activities in the Nordic Seas at these depths [14,16] and because scavenging over the Barents Sea shelves would further reduce their radionuclide content.

Intermediate and deep waters transporting ^{231}Pa and ^{230}Th only exit the Arctic through Fram Strait. There is considerable uncertainty in estimates of the volume transport into and out of the Arctic through Fram Strait, and there may also be seasonal and interannual variability. A recent analysis assigned a southward export of Arctic Intermediate Water of ~ 2 Sv [59]. Export of Eurasian Basin Deep Water from the Arctic has been estimated at ~ 0.7–1.0 Sv [60]. We use a value of 2 Sv for the total export of intermediate/deep waters out of the Arctic (R_{out}) and provide estimates (below) using a range of 1.5–3 Sv (Table 2; Fig. 6). Northward transport of deep water from the Norwegian and Greenland Seas into the Eurasian Basin (R_{in}) has been estimated at ~ 1 Sv [60]. As

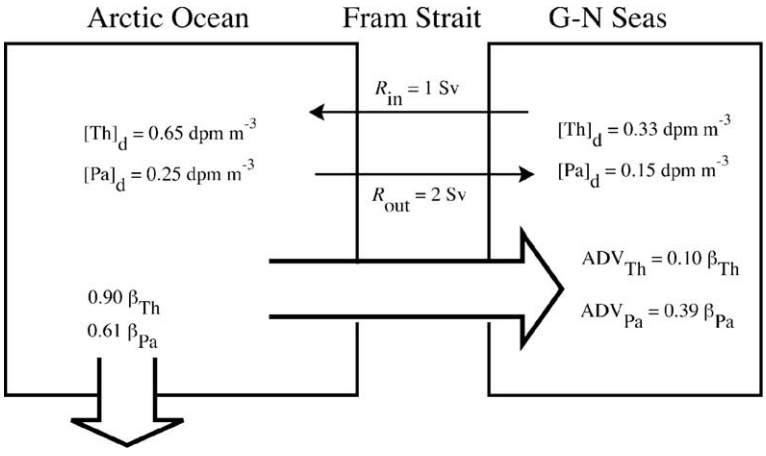

Fig. 6. Scavenging removal and intermediate/deep water transport (ADV) of dissolved ^{231}Pa and ^{230}Th from the Arctic estimated from their respective dissolved activities, in-situ production rates (β_{Th}, β_{Pa}), and horizontal transports (R_{in}, R_{out}) between the Arctic Ocean and the Greenland–Norwegian Seas. For ^{230}Th, ~ 10% of the in-situ production in the central Arctic is exported through Fram Strait and the remaining ~ 90% is removed by particle scavenging and deposited in the underlying sediments. For the less particle-reactive ^{231}Pa, however, ~ 39% produced in the Arctic is exported through Fram Strait into the Greenland–Norwegian Seas before its removal to the sediments.

Table 2
Net export by advection of dissolved ^{230}Th and ^{231}Pa out of the Arctic through Fram Strait compared to the respective radionuclide production rate within the Arctic Ocean (see text for details)

Tracer	β (dpm L^{-1} yr^{-1})	V_{Arctic} (L)	P_{Arctic} (dpm s^{-1})	A_{in} (dpm m^{-3})	A_{out} (dpm m^{-3})	R_{in} (Sv)	R_{out} (Sv)	ADV_{Net} (dpm s^{-1})	ADV_{Net}:P_{Arctic} (%)
^{230}Th	2.52×10^{-5}	1.23×10^{19}	9.8×10^{6}	0.65	0.33	1	2	1.0×10^{6}	10 (7–16)
^{231}Pa	2.33×10^{-6}	1.23×10^{19}	9.1×10^{5}	0.25	0.15	1	2	3.5×10^{5}	39 (25–67)

β: radionuclide production rate; V_{Arctic}: volume of interior Arctic; P_{Arctic}: total production of radionuclide in interior Arctic; A_{in}: average intermediate/deep water radionuclide activity in Arctic; A_{out}: average intermediate/deep water radionuclide activity proximal to Arctic in Greenland–Norwegian Sea; R_{in}: transport of intermediate/deep water through Fram Strait into Arctic; R_{out}: transport of intermediate/deep water through Fram Strait out of Arctic; ADV_{Net}; net advective transport of radionuclide through Fram Strait out of Arctic; Sv=1×10^{6} m^{3} s^{-1}. ADV_{Net}:P_{Arctic} ratios in parenthesis are values calculated using range for R_{out}=1.5–3 Sv.

discussed below, because of the lower dissolved ^{231}Pa and ^{230}Th activities in the Nordic Seas at intermediate/deep water depths [14,16,61], however, advection of ^{231}Pa and ^{230}Th in these deep waters into the Arctic is expected to be lower than export from the Arctic.

Dissolved ^{230}Th activities in Arctic intermediate/deep waters (>1000 m) range from ~ 0.37–1.60 dpm m^{-3} in the Canadian Basin to ~ 0.45–0.69 dpm m^{-3} in the Eurasian Basin [3,28,35,62]. The total volume of the interior Arctic, excluding shelf waters, is 1.23×10^{19} L [35,63] (Table 2). Using a dissolved ^{230}Th activity of 0.65 dpm m^{-3} as representative of intermediate/deep waters and a volume transport of 2 Sv exiting through Fram Strait, the advective transport of dissolved ^{230}Th is 1.30×10^{6} dpm s^{-1}. By comparison, using a ^{230}Th activity of 0.33 dpm m^{-3} at 2000 m (average of 0.39 dpm m^{-3} at 2000 m from J. Scholten, unpublished data, and 0.27 dpm m^{-3} reported for the Norwegian Sea [61]) and a northward transport of intermediate/deep waters of 1 Sv through Fram Strait results in 3.3×10^{5} dpm s^{-1} into the Arctic. The net advective export of dissolved ^{230}Th from the Arctic through Fram Strait (ADV_{Th}) is thus 0.97×10^{6} dpm s^{-1}. The in-situ production rate of ^{230}Th for the volume of water in the interior Arctic (1.23×10^{19} L) is 9.8×10^{6} dpm s^{-1} (Table 2). This implies that only ~ 10% of dissolved ^{230}Th produced in the central Arctic is exported through Fram Strait (7–16% using a range of 1.5–3 Sv for the southward flow through Fram Strait; Table 2; Fig. 6).

Of the ~ 90% of dissolved ^{230}Th remaining in the Arctic (Fig 6), approximately one-third (38% on average; [29]) is scavenged to central basin sediments. Thus, boundary scavenging of ^{230}Th must be occurring in the Arctic such that the remaining two-thirds of the dissolved ^{230}Th not exported are removed at the margins. This conclusion may seem at odds with previous studies that indicate ^{230}Th is removed locally in other ocean basins and not subject to boundary scavenging [4,5,9]. We attribute this to the unique conditions of the Arctic Ocean that should enhance boundary scavenging; specifically, rapid lateral mixing between the margin and interior waters of this relatively small ocean basin; the regional extremes in particle flux; and, the high proportion of the sedimenting lithogenic particles that may account for the low and comparable $^{231}Pa_{xs}/^{230}Th_{xs}$ values in both basin and margin sediments [21].

For ^{231}Pa, dissolved activities in the interior Arctic intermediate/deep waters range from ~ 0.10–0.60 dpm m^{-3} in the Canadian Basin to ~ 0.15–0.40 dpm m^{-3} in the Eurasian Basin [3,28,35]. With a dissolved ^{231}Pa activity of 0.25 dpm m^{-3} in Arctic intermediate/deep waters and a southward flow of 2 Sv through Fram Strait, the advective transport is 5.0×10^{5} dpm s^{-1}. By comparison, using a dissolved ^{231}Pa activity of 0.15 dpm m^{-3} at 1700 m (J. Scholten, unpublished data) and an intermediate/deep water volume transport of 1 Sv northward through Fram Strait results in 1.5×10^{5} dpm s^{-1} into the Arctic. The net advective export of dissolved ^{231}Pa from the Arctic through Fram Strait (ADV_{Pa}) is estimated to be 3.5×10^{5} dpm s^{-1}. The in-situ production rate of ^{231}Pa for the volume of water in the interior Arctic is 9.1×10^{5} dpm s^{-1} (Table 2). This implies that ~ 39% of dissolved ^{231}Pa produced in the central Arctic is exported through Fram Strait (25–67% using a range of 1.5–3 Sv for the southward flow through Fram Strait; Table 2; Fig. 6), with the remaining 61% removed by particle scavenging within the Arctic (Fig. 6). A similar conclusion has been reported with regard to

the meridional transport of ^{231}Pa in the Atlantic [13,16,17].

The validity of the above estimates for water column transports of dissolved ^{231}Pa and ^{230}Th can be tested against the observed Arctic surface sediment $^{231}Pa_{xs}/^{230}Th_{xs}$ ratios. Because there is no apparent $^{231}Pa_{xs}/^{230}Th_{xs}$ fractionation between the margins and interior basins (Fig. 2), we expect surface sediments to bear a $^{231}Pa_{xs}/^{230}Th_{xs}$ ratio $=(0.61\beta_{Pa})/(0.90\beta_{Th})=0.063$, where β is the production rate (Table 2). This result is in excellent agreement with the observed basinwide $^{231}Pa_{xs}/^{230}Th_{xs}$ ratio of 0.063 ± 0.014. In addition, this water column evidence supports our suggestion that the observed low surface sediment $^{231}Pa_{xs}/^{230}Th_{xs}$ ratios are unlikely to be significantly affected by bioturbation. As noted above, a further implication of the lack of basin-margin fractionation is that scavenging of ^{231}Pa and ^{230}Th must be comparable in both the central Arctic and at the margins.

These results imply that, due to the similar residence time of dissolved ^{231}Pa and intermediate/deeper waters, nearly half of the in-situ production of this tracer is exported from the Arctic. This explains the uniformly low surface sediment $^{231}Pa_{xs}/^{230}Th_{xs}$ ratios (~ 0.06) and lack of $^{231}Pa_{xs}/^{230}Th_{xs}$ fractionation between the basin interior and marginal areas. Contrary to previous work [54], we find only a minimal export of ^{230}Th out of the Arctic, which further implies that, in addition to ^{231}Pa, ^{230}Th is removed by boundary scavenging in the Arctic due to its significant removal at/near the basin boundary.

5. Conclusions

The distribution of surface sediment $^{231}Pa_{xs}/^{230}Th_{xs}$ ratios in the Arctic provides new insight as to the relative importance of scavenging removal and horizontal transport in redistributing these particle-reactive tracers between the low productivity, permanently ice-covered, interior basins and the seasonally high particle flux margins. On a basin-wide scale, low surface sediment $^{231}Pa_{xs}/^{230}Th_{xs}$ ratios are interpreted as resulting from chemical fractionation of ^{231}Pa and ^{230}Th in the water column and preferential export of ^{231}Pa out of the Arctic Ocean. Whereas a significant fraction (~ 39%) of ^{231}Pa produced in-situ is exported from the Arctic, essentially all (~ 90%) of ^{230}Th produced in-situ are removed within the Arctic by particle scavenging. Export of the intermediate/deep interior waters through Fram Strait limits the extent to which ^{231}Pa can accumulate in high particle flux marginal sediments by boundary scavenging. Bioturbation is unlikely to be the primary cause of the uniformly low surface sediment (0–1 cm) $^{231}Pa_{xs}/^{230}Th_{xs}$ ratios across the Arctic Ocean, though it may be important at the extremely low sedimentation rates characteristic of the interior Canadian Basin. The sizable export of ^{231}Pa relative to that of ^{230}Th accounts for both the low sediment $^{231}Pa_{xs}/^{230}Th_{xs}$ ratios and lack of basin-margin fractionation, despite there being significant boundary scavenging of both ^{231}Pa and ^{230}Th in the Arctic, a situation unique to this ocean basin. A further implication is that there is likely to be export of other similarly reactive radionuclides (e.g., ^{10}Be, Pu isotopes) from the Arctic.

Acknowledgments

We thank the Captain and crew of the *C.C.G.S Louis S. St. Laurent* and *U.S.C.G.C. Polar Sea*, Chief Scientists Knut Aagaard and Eddy Carmack, and Rick Nelson and the late Kathy Ellis for assistance with sample collection, processing, and logistics. We thank the Captain and crew of the *U.S.G.C Healy* and Jackie Grebmeier and Lee Cooper for providing samples from the SBI-II 2002 cruise. Michiel Rutgers van der Loeff, an anonymous reviewer and Martin Frank provided insightful and constructive comments. This work was funded by the NSF (OCE-9730257, OPP-0002313, OCE-9731127, EAR-9712037, and OPP-0124917), the ONR (Young Investigator Award N00014-96-1-0685 to SBM), and the ROC Taiwan NSC (91- 2116-M-006004, 92-2116-M-002013, and PPAEU to CCS).

References

[1] M.P. Bacon, R.F. Anderson, Distribution of thorium isotopes between dissolved and particulate forms in the deep sea, J. Geophys. Res. 87 (1982) 2045–2056.
[2] Y. Nozaki, T. Nakanishi, ^{231}Pa and ^{230}Th in the open ocean water column, Deep-Sea Res. 32 (1985) 1209–1220.
[3] H.N. Edmonds, S.B. Moran, J.A. Hoff, J.N. Smith, R.L. Edwards, Protactinium-231 and Thorium-230 abundances and

high scavenging rates in the Western Arctic Ocean, Science 280 (1998) 405–407.
[4] R.F. Anderson, M.P. Bacon, P.G. Brewer, Removal of ^{230}Th and ^{231}Pa at ocean margins, Earth Planet. Sci. Lett. 66 (1983) 73–90.
[5] R.F. Anderson, M.P. Bacon, P.G. Brewer, Removal or ^{230}Th and ^{231}Pa from the open ocean, Earth Planet. Sci. Lett. 62 (1983) 7–23.
[6] R.F. Anderson, Y. Lao, W.S. Broecker, S.E. Trumbore, H.J. Hofmann, W. Wolfli, Boundary scavenging in the Pacific Ocean: a comparison of ^{10}Be and ^{231}Pa, Earth Planet. Sci. Lett. 96 (1990) 287–304.
[7] D.W. Spencer, M.P. Bacon, P.G. Brewer, Models of the distribution of ^{210}Pb in a section across the North Atlantic Ocean, J. Mar. Res. 39 (1981) 119–138.
[8] M.P. Bacon, D.W. Spencer, P.G. Brewer, ^{210}Pb/^{226}Ra and ^{210}Pb/^{210}Po disequilibria in seawater and suspended matter, Earth Planet. Sci. Lett. 32 (1976) 277–296.
[9] M.P. Bacon, Tracers of chemical scavenging in the ocean: boundary effects and largescale chemical fractionation, Philos. Trans. R. Soc. London, Ser. A 325 (1988) 147–160.
[10] H.-S. Yang, Y. Nozaki, H. Sakai, A. Masuda, The distribution of ^{230}Th and ^{231}Pa in the deep-sea surface sediments of the Pacific Ocean, Geochim. Cosmochim. Acta 50 (1986) 81–89.
[11] G.B. Shimmield, J.W. Murray, J. Thomson, M.P. Bacon, R.F. Anderson, N.B. Price, The distribution and behaviour of ^{230}Th and ^{231}Pa at an ocean margin, Geochim. Cosmochim. Acta 50 (1986) 2499–2507.
[12] Y. Lao, R.F. Anderson, W.S. Broecker, Boundary scavenging and deep-sea sediment dating: constraints from excess ^{230}Th and ^{231}Pa, Paleoceanography 7 (1992) 783–798.
[13] E.-F. Yu, R. Francois, M.P. Bacon, Similar rates of modern and last-glacial ocean thermohaline circulation inferred from radiochemical data, Nature 379 (1996) 689–694.
[14] S.B. Moran, M.A. Charette, J.A. Hoff, R.L. Edwards, W.M. Landing, Distribution of ^{230}Th in the Labrador Sea and its relation to ventilation, Earth Planet. Sci. Lett. 150 (1997) 151–160.
[15] S.B. Moran, C.-C. Shen, S.E. Weinstein, L.H. Hettinger, J.A. Hoff, H.N. Edmonds, R.L. Edwards, Constraints on deep water age and particle flux in the equatorial and South Atlantic Ocean based on seawater ^{231}Pa and ^{230}Th data, Geophys. Res. Lett. 28 (2001) 3437–3440.
[16] S.B. Moran, C.-C. Shen, H.N. Edmonds, S.E. Weinstein, J.N. Smith, R.L. Edwards, Dissolved and particulate ^{231}Pa and ^{230}Th in the Atlantic Ocean: constraints on intermediate/deep water age, boundary scavenging and ^{231}Pa/^{230}Th fractionation, Earth Planet. Sci. Lett. 203 (2002) 999–1014.
[17] O. Marchal, R. Francois, T.F. Stocker, F. Joos, Ocean thermohaline circulation and sedimentary ^{231}Pa/^{230}Th ratio, Paleoceanography 15 (2000) 625–641.
[18] E.-F. Yu, R. Francois, M.P. Bacon, A.P. Fleer, Fluxes of ^{230}Th and ^{231}Pa to the deepsea: implications for the interpretation of excess ^{230}Th and ^{231}Pa/^{230}Th profiles in sediments, Earth Planet. Sci. Lett. 191 (2001) 219–230.
[19] L.D. Guo, M. Chen, C. Gueguen, Control of Pa/Th ratio by particulate chemical composition in the ocean, Geophys. Res. Lett. 29 (20) (2002), doi:10.1029/2002GL015666.
[20] S. Luo, T.-L. Ku, On the importance of opal, carbonate, and lithogenic clays in scavenging and fractionating ^{230}Th, ^{231}Pa, and ^{10}Be in the ocean, Earth Planet. Sci. Lett. 220 (2004) 201–211.
[21] S. Luo, T.-L. Ku, Oceanic ^{231}Pa/^{230}Th ratio influenced by particle composition and remineralization, Earth Planet. Sci. Lett. 167 (1999) 183–195.
[22] H.L. Andersen, R. Francois, S.B. Moran, Experimental evidence for differential adsorption of Th and Pa on different particle types in seawater, Eos, Trans.-Am. Geophys. Union 73 (1992) 270.
[23] Z. Chase, R.F. Anderson, M.Q. Fleisher, P.W. Kubik, The influence of particle composition and particle flux on scavenging of Th, Pa and Be in the ocean, Earth Planet. Sci. Lett. 204 (2002) 215–229.
[24] H.J. Walter, M.M. Rutgers van der Loeff, H. Hoeltzen, Enhanced scavenging of ^{231}Pa relative to ^{230}Th in the South Atlantic south of the Polar Front: implications for the use of the ^{231}Pa/^{230}Th ratio as a paleoproductivity proxy, Earth Planet. Sci. Lett. 149 (1997) 85–100.
[25] T. Asmus, M. Frank, C. Koschmieder, N. Frank, R. Gersonde, G. Kuhn, A. Mangini, Variations of biogenic particle flux in the southern Atlantic section of the Subantarctic Zone during the Late Quaternary evidence from sedimentary $^{231}Pa_{ex}$ and $^{230}Th_{ex}$, Mar. Geol. 159 (1999) 63–78.
[26] T.-L. Ku, W.S. Broecker, Rates of sedimentation in the Arctic Ocean, Prog. Oceanogr. 4 (1967) 95–104.
[27] R. Finkel, S. Krishnaswami, D.L. Clark, ^{10}Be in Arctic Ocean sediments, Earth Planet. Sci. Lett. 35 (1977) 199–204.
[28] J.C. Scholten, M.M. Rutgers van der Loeff, A. Michel, Distribution of ^{230}Th and ^{231}Pa in the water column in relation to the ventilation of deep Arctic basins, Deep-Sea Res. II 42 (6) (1995) 1519–1531.
[29] C.A. Huh, N.G. Pisias, J.M. Kelly, T.C. Maiti, A. Grantz, Natural radionuclides and plutonium in sediments from the Western Arctic Ocean: sedimentation rates and pathways of radionuclides, Deep-Sea Res. II 44 (8) (1997) 1725–1744.
[30] J.H. Chen, R.L. Edwards, G.J. Wasserburg, ^{238}U, ^{234}U and ^{232}Th in seawater, Earth Planet. Sci. Lett. 80 (1986) 241–251.
[31] C.-C. Shen, R.L. Edwards, H. Cheng, R.B. Dorale, R.B. Thomas, S.B. Moran, S.E. Weinstein, H.N. Edmonds, Uranium and thorium isotopic and concentration measurements by magnetic sector inductively coupled plasma mass spectrometry, Chem. Geol. 185 (2002) 165–178.
[32] C.-C. Shen, H. Cheng, R.L. Edwards, S.B. Moran, H.N. Edmonds, J.A. Hoff, R.B. Thomas, Measurement of attogram quantities of ^{231}Pa in dissolved and particulate fractions of seawater by isotope dilution thermal mass spectrometry, Anal. Chem. 75 (2003) 1075–1079.
[33] G.M. Henderson, R.F. Anderson, The U-series toolbox for paleoceanography, Rev. Mineral. Geochem. 52 (2003) 493–531.

[34] E.-F. Yu, Variations in the particulate flux of ^{230}Th and ^{231}Pa and paleoceanographic applications of the ^{231}Pa/^{230}Th Ratio, Doctoral dissertation, Woods Hole Oceanographic Institution–Massachusetts Institute of Oceanography, 1994.
[35] H.N. Edmonds, S.B. Moran, H. Cheng, R.L. Edwards, ^{230}Th and ^{231}Pa in the Arctic Ocean: implications for particle fluxes and basin-scale Th/Pa fractionation, Earth Planet. Sci. Lett. 227 (2004) 155–167.
[36] M. Roy-Barman, J.H. Chen, G.J. Wasserburg, ^{230}Th–^{232}Th systematics in the central Pacific Ocean: the sources and fates of thorium, Earth Planet. Sci. Lett. 139 (1996) 351–363.
[37] S. Vogler, J. Scholten, M.M. Rutgers van der Loeff, A. Mangini, ^{230}Th in the eastern North Atlantic: the importance of water mass ventilation in the balance of ^{230}Th, Earth Planet. Sci. Lett. 156 (1997) 61–74.
[38] L.M. Clough, W.G. Ambrose, J.K. Cochran, C. Barnes, P.E. Renaud, R.C. Aller, Infaunal density, biomass and bioturbation in the sediments of the Arctic Ocean, Deep-Sea Res. II 44 (8) (1997) 1683–1704.
[39] J.N. Smith, S.B. Moran, R.W. MacDonald, Shelf-basin interactions in the Arctic Ocean based on ^{210}Pb and Ra isotope tracer distributions, Deep-Sea Res. I 50 (2003) 397–416.
[40] Y. Nozaki, J.K. Cochran, K.K. Turekian, G. Keller, Radiocarbon and ^{210}Pb distribution in submersible-taken deep-sea cores from project FAMOUS, Earth Planet. Sci. Lett. 34 (1977) 167–173.
[41] T.-H. Peng, W.S. Broecker, G. Kipphut, N. Shackleton, Benthic mixing in deep sea cores as determined by ^{14}C dating and its implications regarding climate stratigraphy and the fate of fossil fuel CO_2, in: N.R. Anderson, A. Malahoff (Eds.), Fate of Fossil Fuel CO_2 in the Oceans, Plenum Press, 1977, pp. 355–373.
[42] D.V. Subba Rao, T. Platt, Primary production of Arctic waters, Pol. Biol. 3 (1984) 191–201.
[43] J.J. Walsh, Arctic carbon sinks: present and future, Glob. Biogeochem. Cycles 3 (1989) 393–411.
[44] P.A. Wheeler, M. Gosselin, E.B. Sherr, D. Thibault, D.L. Kirchman, R. Benner, T.E. Whitledge, Active cycling of organic carbon in the central Arctic ocean, Nature 380 (1996) 697–699.
[45] P.A. Wheeler, J.M. Watkins, R.L. Hansing, Nutrients, organic carbon and organic nitrogen in the upper water column of the Arctic Ocean: implications for the sources of dissolved organic carbon, Deep-Sea Res. II 44 (8) (1997) 1571–1592.
[46] M. Gosselin, M. Levasseur, P.A. Wheeler, B.C. Booth, R.A. Horner, New measurements of phytoplankton and ice algal production in the Arctic Ocean, Deep-Sea Res. II 44 (8) (1997) 1623–1644.
[47] B.T. Hargrave, B. von Bodungen, P. Stoffyn-Egli, P.J. Mudie, Seasonal variability in particle sedimentation under permanent ice cover in the Arctic Ocean, Cont. Shelf Res. 14 (1994) 279–293.
[48] S.B. Moran, K.M. Ellis, J.N. Smith, ^{234}Th/^{238}U disequilibria in the central Arctic Ocean: implications for particulate organic carbon export, Deep-Sea Res. II 44 (1997) 1593–1606.
[49] S.B. Moran, J.N. Smith, ^{234}Th as a tracer of scavenging and particle export in the Beaufort Sea, Cont. Shelf Res. 20 (2000) 153–167.
[50] S.M. Trimble, M. Baskaran, D. Porcelli, Scavenging of thorium isotopes in the Canada Basin of the Arctic Ocean, Earth Planet. Sci. Lett. 222 (2004) 915–932.
[51] M. Baskaran, P.W. Swarzenski, D. Porcelli, Role of colloidal material in the removal of ^{234}Th in the Canada Basin of the Arctic Ocean, Deep-Sea Res. I 50 (2003) 1353–1373.
[52] W.M. Smethie, P. Schlosser, T.S. Hopkins, G. Bonisch, Renewal and circulation of intermediate waters in the Canadian Basin observed on the Scicex-96 cruise, J. Geophys. Res. 105 (2000) 1105–1121.
[53] E.C. Carmack, K. Aagaard, J.W. Swift, R.W. MacDonald, F.A. McLaughlin, E.P. Jones, R.G. Perkin, J.N. Smith, K.M. Ellis, L. Kilius, Changes in temperature and tracer distributions within the Arctic Ocean: results from the 1994 Arctic Ocean section, Deep-Sea Res. II 44 (1997) 1487–1502.
[54] M.P. Bacon, C.-A. Huh, R.M. Moore, Vertical profiles of some natural radionuclides over the Alpha Ridge, Arctic Ocean, Earth Planet. Sci. Lett. 95 (1989) 15–22.
[55] D.W.R. Wallace, P. Schlosser, M. Krysell, G. Bonisch, Halocarbon ratio and tritium/^{3}He dating of water masses in the Nansen Basin, Arctic Ocean, Deep-Sea Res. I 39 (1992) S435–S458.
[56] G. Bonisch, P. Schlosser, Deep water formation and exchange rates in the Greenland/Norwegian seas and Eurasian Basin of the Arctic Ocean derived from tracer balances, Prog. Oceanogr. 35 (1995) 29–52.
[57] H.G. Ostlund, G. Possnert, J.H. Swift, Ventilation rate of the deep Arctic Ocean from carbon 14 data, J. Geophys. Res. 92 (1987) 3769–3777.
[58] R.W. MacDonald, E.C. Carmack, D.W.R. Wallace, Tritium and radiocarbon dating of Canada Basin deep waters, Science 259 (1993) 103–104.
[59] R.W. MacDonald, et al., Contaminants in the Canadian Arctic: 5 years of progress in understanding sources, occurrence and pathways, Sci. Total Environ. 254 (2000) 93–234.
[60] C. Heinze, P. Schlosser, K.P. Koltermann, J. Meincke, A tracer study of the deep water renewal in the European polar seas, Deep-Sea I 37 (9) (1990) 1425–1453.
[61] S.B. Moran, J.A. Hoff, K.O. Buesseler, R.L. Edwards, High precision ^{230}Th and ^{232}Th in the Norwegian Sea and Denmark by thermal ionization mass spectrometry, Geophys. Res. Lett. 22 (19) (1995) 2589–2592.
[62] J.K. Cochran, D.J. Hirschberg, H.D. Livingston, K.O. Buesseler, R.M. Key, Natural and artificial radionuclide distributions in the Nansen Basin, Arctic Ocean: scavenging rates and circulation timescales, Deep-Sea Res. II 42 (1995) 1495–1517.
[63] M. Jakobsson, Hypsometry and volume of the Arctic Ocean and its constituent seas, Geochem. Geophys. Geosyst. 3 (5) (2002), doi:10.1029/2001GC000302.
[64] N. Nørgaard-Pedersen, R.F. Spielhagen, H. Erlenkeuser, P.M. Grootes, J. Heinemeier, J. Knies, Arctic Ocean during the last glacial maximum: Atlantic and polar domains of surface water mass distribution and ice cover, Paleoceanography 18 (3) (2003) 1063.

[65] N. Nørgaard-Pedersen, R.F. Spielhagen, J. Thiede, H. Kassens, Central Arctic surface ocean environment during the past 80,000 years, Paleoceanography 13 (2) (1998).
[66] R. Stein, C. Schubert, C. Vogt, D. Fuetterer, Stable isotope stratigraphy, sedimentation rates and salinity changes in the late Pleistocene to Holocene eastern central Arctic Ocean, Mar. Geol. 119 (1994) 333–355.
[67] M. Weinelt, Veränderungen der Öberflächenzirkulation im Europäischen Nordmeer während der letzten 60.000 Jahre-Hinweise aus stabilen Isotopen, Report SFB 313, Kiel University, Kiel, 1993, p. 1106.